



Methodological Advancements for Brain Tumour Segmentation in Magnetic Resonance Imaging: A Survey

Mansi Kajal¹ * and Pulkit Dwivedi²

¹ Apex Institute of Technology (CSE), Chandigarh University, India

² Indian Institute of Information Technology, Lucknow, India

Abstract. Brain tumour segmentation is a widely explored area of research within both medical and engineering domains, particularly focusing on Magnetic Resonance Imaging (MRI) as the primary modality for detection. Computer-aided diagnosis (CADx) systems play a pivotal role in automating the detection and classification of brain tumours from MRI images. A crucial component of CADx systems is the segmentation module, responsible for precisely delineating tumour regions. Accurate segmentation, with sub-pixel precision, is essential for determining tumor size, and location, and facilitating image-guided surgical procedures. In recent years, numerous methods have emerged for segmenting brain tumours from MRI images. This paper presents a comprehensive survey of state-of-the-art segmentation methods, along with an overview of datasets commonly used for method development and the evaluation metrics employed. By offering a consolidated overview, this study serves as a valuable resource for novice researchers entering this field and provides updated information for researchers already engaged in brain tumour segmentation research.

Keywords: Brain tumour detection, Medical Image Analysis, Image segmentation, Magnetic Resonance Imaging, Deep learning, Convolutional Neural Networks

1 Introduction

A brain tumor is a mass of either malignant or benign growth that develops in or around the brain. While benign tumors are non-cancerous and do not infiltrate neighboring tissues, malignant tumors are cancerous, growing and spreading uncontrollably [1, 2]. Malignant brain tumors are notably aggressive and considered among the deadliest cancers, with increasing incidence and prevalence [3]. According to the World Health Organization (WHO), as of 2021, the global prevalence and incidence of brain tumors were reported at 700,000 and 84,170 respectively³.

Brain tumors are categorized by different levels of aggressiveness, graded from I to IV [4].

Table 1 summarizes brain tumor subtypes according to their aggressiveness levels.

Table 1: Brain tumor subtypes as per WHO Grades

Brain Tumor Types	Subtypes	Grades	Features
Benign	Pilocytic Astrocytoma	I	Slow-growing, cerebrum growth
	Low-grade Astrocytoma	II	Slow-growing, rare spread, common in men and women
Malignant	Anaplastic Astrocytoma	III	Faster growth, more aggressive
	Glioblastoma	IV	Rapid growth, less common in children

* Corresponding author

³ <https://www.cancer.net/search/site/brain%20tumour>

Various imaging techniques, including Positron Emission Tomography (PET) [5], Computed Tomography (CT) [6], and Magnetic Resonance Imaging (MRI) [7], are utilized for brain tumor detection. Among these, MRI is preferred due to its detailed soft tissue visualization capabilities. While MRI is the preferred modality, interpreting MRI scans for brain tumors requires significant training and expertise, often leading to inter- and intra-observer bias, detection errors, and prolonged turnaround times. Hence, Computer-Aided Diagnosis (CADx) systems are essential for interpreting MRI scans and detecting abnormalities. These systems have evolved significantly, transitioning from early rule-based image processing methods to more advanced machine learning-based approaches [8–10].

This paper provides a systematic overview of the methodological advancements in brain tumor segmentation (BTS) methods over the years. It covers data collection protocols, brain anatomy, MRI modality, commonly used datasets, evaluation metrics, and a detailed description of BTS systems.

The rest of the paper is organized as follows: Section 2 presents the data collection protocol, followed by descriptions of brain anatomy (Section 3) and MRI modality (Section 4). Section 5 summarizes commonly used datasets, while Section 6 discusses evaluation metrics. A categorical description of BTS systems is presented in Section 7. Finally, the paper concludes in Section 8.

2 Data Collection

To comprehensively identify relevant publications, primary searches were conducted from 2005 to 2022 across various databases, including ACM Digital Library, IEEE Xplore, ScienceDirect, and Springer. Additionally, secondary searches were performed to augment the primary results. The bibliography of identified studies was meticulously reviewed and considered. In total, 642 primary searches and 100 secondary searches were conducted, resulting in a collection of 742 papers.

Initially, papers were screened based on their titles, resulting in the selection of 598 papers and the rejection of 144 papers. Subsequently, abstracts were reviewed, leading to the selection of 300 papers and the rejection of 298 papers. Finally, based on full-text assessments, 118 papers were chosen for inclusion in this study due to their overall relevance to the topic.

This comprehensive data collection process ensured the inclusion of a diverse range of relevant research publications for the synthesis and analysis presented in this paper.

3 Brain Anatomy

The brain serves as the central control center for the body, interpreting external stimuli and orchestrating various bodily functions. It comprises three major regions: the cerebrum, cerebellum, and brainstem [11], as illustrated in Figure 1.

1. **Cerebrum:** The cerebrum, the largest portion of the brain, consists of the right and left hemispheres. It is responsible for tasks such as comprehension, touch, vision, hearing, communication, logical reasoning, learning, and precise movement. The surface of the cerebrum, known as the cerebral cortex, consists of white matter and gray matter, housing around 400 million neurons organized in layers. Each hemisphere controls the opposite side of the body, and stroke or injury to one hemisphere can lead to paralysis or weakness on the opposite side [12].

– **Frontal lobe:** The largest lobe, responsible for emotions, personality, decision-making, planning, problem-solving, language production (Broca's area), and voluntary movement (motor strip). It also governs self-awareness, intelligence, and attention.

– **Parietal lobe:** Located at the top of the brain, it aids in object identification, language comprehension (Wernicke's area), interpretation of sensory information (touch, temperature, pain), and spatial perception.

– **Occipital lobe:** Positioned at the back of the brain, it processes visual information, including interpretation of color, brightness, and motion.

– **Temporal lobe:** Situated on the sides of the brain, it handles short-term memory, language comprehension, smell, hearing, organization, and sequencing.

2. **Cerebellum:** Located beneath the cerebrum, the cerebellum is a small structure about the size of a fist. Its main functions include coordination of muscle movements, maintenance of posture, and regulation of balance [13].

3. **Brainstem:** Situated at the base of the brain, the brainstem connects the cerebrum to the spinal cord and serves as a relay station for various bodily functions. It regulates vital automatic processes such as breathing, heartbeat, body temperature, digestion, sneezing, coughing, vomiting, and the circadian rhythm governing the sleep-wake cycle [14].

Understanding the intricate anatomy and functions of the brain is crucial for interpreting brain imaging data and diagnosing neurological disorders accurately.

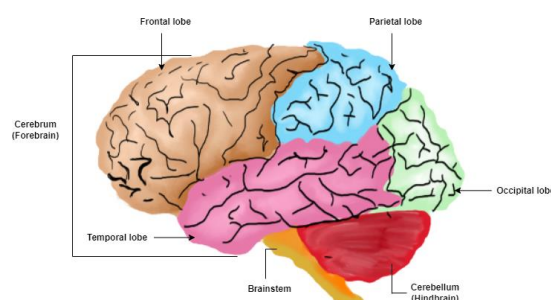


Fig. 1: Brain Anatomy: cerebrum, cerebellum, and brainstem

4 MRI (Magnetic Resonance Imaging)

Although it was initially noticed in the 1930s, medical imaging technology was not developed until the 1970s. Nuclear magnetic resonance (NMR) is the effect of spinning atoms. Patient's thought the word "nuclear" was insulting, so it was renamed MRI. Paul Lauterbur demonstrated NMR imaging for the first time in 1973. He changed the field strength, causing individual particles to fluctuate and allowing him to piece together an image.

MRI uses the magnetic properties of the brain to generate accurate high-resolution images instead of utilising X-rays. An MRI scan of the body is used to determine the size of a brain tumour. To identify and treat internal organ problems, radiology uses medical imaging. Any portion of the body in any orientation is imaged with a magnetic resonance imaging (MRI) scanner (e.g., the head, ligaments and tendons, limbs, belly, etc.). Compared to CT, MRI provides a greater soft tissue contrast and can differentiate amongst lipid, water, muscles, as well as other soft tissue (CT is usually better at imaging bones). Professionals can use these images to diagnose a variety of diseases and disorders and to deliver information. The most typical method used in neurology to view the brain and other cranial structures in depth is an MRI scan. It aids in the understanding of anatomy in three planes: axial, sagittal, and transverse [15]. MRI is a very safe procedure that most people can have. In some circumstances, however, an MRI scan may not be required. If you feel you have metal in your body, you should tell your doctor before undergoing an MRI scan.

There are different types of MRIs such as: FMRI, S-MRI, DWI MRI. 1) F-MRI (Functional Magnetic Resonance Imaging): This technique uses blood flow variations to evaluate brain activity. 2) DWI MRI (Diffusion Weighted Imaging MRI): It is a method to evaluate the micro architecture of the human body and functionality of the molecules of the body. 3) S-MRI (Structural MRI): Brain anatomy and diseases can be seen with S-MRI imaging. In order to address brain pathology, the suggested essay will focus on S-MRI. S-MRI captures tissue responses in a variety of ways, resulting in images with varying biological information.

The following are some examples of S-MRI techniques:

1. **FLAIR MRI:** A Magnetic resonance imaging heartbeat sequential that reduces fluid (primarily Cerebrospinal fluid) while increasing edema.
2. **T1w MRI:** A conventional MRI pulse sequence is used to capture variations in tissue lengthwise T1 relaxation time (the continual time needed for excited protons to go back to balance).
3. **MRI with T1Gd:** Gadolinium, is a contrast enhanced, which is introduced into the body, followed by the T1 sequence. This contrast enhancer reduces T1 time, making blood vessels and illnesses like tumours appear brighter.
4. **T2w MRI:** A conventional MRI pulse sequence is used to capture tissue transverse relaxation time (T2) variations.

Diffusion Weighted Image (DWI) MRI: To evaluate the diffusion of water particles within cell voxels, an MRI imaging technique is used. DWI is widely used to detect hyperintensities. It's involved in MRI to show the greatest contrast and for highlighting the tissues injury within the cerebral infarct and reported with the sensitivity and the specificity in the results of the datasets. It is a technical tool for evolution and the application is increasing day by day.

F-MRI (Functional MRI): The science of functional MRI imaging has advanced significantly since Belliveau et al. initial publication, which showed changes in the brain's MRI imaging signals that are connected to blood flow [16]. In 1990, Ogawa et al. described the BOLD contrast effect, and in 1992, two research groups used BOLD contrast for functional MRI imaging of the brain [17]. A extremely different performance MRI imaging is now.

For a long time, MRI has been recognised as a reliable tool for tracking pedesis (brownian motion), also known as widely used in neuroscientific search and is an important part of the surgical strategic planning for brain tumours [18] diffusion. Moseley et al. were the first to recognise that acute cerebral infarction may be seen in 1990. Methods of the Diffusion imaging, including as DTI (diffusion tensor imaging) and diffusion or MRI tractography, can be used to look at the connections and structure of healthy and diseased brains, as well as suspected strokes [19]. Additionally, image analysis during the first throw of a diamagnetic dissimilarity can be used to do the measurement of blood flow in target tissues (Perfusion imaging). material or using arterial spin labelling to provide a "virtual" contrast agent [20, 21]. Perfusion imaging, when used in conjunction with diffusion imaging, provides for a thorough examination of suspected strokes, tumours, and other illnesses [22–24]. All the available brain imaging modalities are compared in Table 2.

5 Datasets

Most of the research in development of BTS systems rely on standard publicly available datasets. BRATS datasets are amongst the most commonly used for the BTS methods. BRATS datasets

Table 2: Comparison of different modalities

Modality	Founder	Year	Spectrum	Use	Pros	Cons
MRI [7]	Raymond Damadin	1997	Magnetic Waves	Detailed pictures of any part of the body	<ul style="list-style-type: none"> Takes images of body. Soft tissue contrast is better (\$1000- with MRI than \$1500) CT. 	<ul style="list-style-type: none"> Takes time more of the internal organs MRI is expensive
PET [5]	Edward Hoffman	J. 1997	Radiotracers	<ul style="list-style-type: none"> Double diagnostic clarity Non-disruptive 	<ul style="list-style-type: none"> Slow growing (less than 7mm) Less active tumours 	<ul style="list-style-type: none"> may not absorb much tracer
CT [6]	Godfrey Hounsfield	1972	Ionizing radiation	Detecting dis-	<ul style="list-style-type: none"> Simultaneously examine blood vessels Highly accurate, metal non-invasive. 	<ul style="list-style-type: none"> Breath hold- ing which some patients cannot manage. Artefact is common eg., clips.
Ultrasound [25]	Donald and engineer Tom Brown	1950	Sound waves	<ul style="list-style-type: none"> During pregnancy, examine procedure safer and development techniques. Identify gall-bladder disease. Analyse flow of blood 	<ul style="list-style-type: none"> Ionizing radiation, making the number of fre- Painless 	<ul style="list-style-type: none"> With increased depth, a lower female reproductive organs than diagnostic is needed for proper imaging. Bone blocks US waves.
X-Rays [26]	W.C. Rontgen	1895	Ionizing radiation	checking the fractures (broken bones)	<ul style="list-style-type: none"> Non-invasive and pain less Medium image quality 	<ul style="list-style-type: none"> X-rays are linked to a slightly increased risk of cancer Bones absorb the radiation

Table 3: Comparison of standard datasets

Dataset	Year	Source	Modalities	Size	Resolution	Image Format	References
MICCAI BRATS	2021	CBICA	T1, T1-GD, T2, T2-FLAIR	13GB	240*240*155*4	DICOM	[27, 28]
BRATS	2020	CBICA	T1, T1-GD, T2, T2-FLAIR	8GB	240*240*155*4	.png	[30, 31]
IRMA	2020			1GB			[84]
MICCAI BRATS	2019	CBICA	T1, T1-GD, T2, T2-FLAIR	5GB	5k*5k*pixels	.png	[85, 87, 88, 95]
LGG-tumor segmentation	2019	TCGA-LGG	FLAIR	1GB			[89]
BRATS	2018	CBICA	T1, T1c, T2 and FLAIR	1GB	1x1x1 mm isotropic resolution	.png	[90, 91, 91, 92, 94, 95, 103]
Figshare	2017				561*352 pixels		[96-99]
BRATS	2017	CBICA	T1, T1-GD, T2, T2-FLAIR		3D (256 × 256 × 140) pixels	.png	[37, 98, 106]
BRATS	2016	CBICA	T1, T1-GD, T2, T2-FLAIR		isotropic resolution (1.125 × 1.125 × 1.125 mm ³ voxel size)	.png	[36, 36]
BRATS	2015	CBICA	T1, T1-GD, T2, T2-FLAIR		1*1*1 mm	.png	[37, 101-106]
BRATS	2013	CBICA	T1, T1-GD, T2, T2-FLAIR			.png	[38, 102, 107, 108]
BRATS	2012	CBICA	T1, T1-GD, T2, T2-FLAIR		640 × 480 pixels	.png	[39, 109-111]

includes four MRI modalities with corresponding ground truth. BRATS datasets are available in different forms like, BRATS 2012, BRATS 2013, BRATS 2014, BRATS 2015, BRATS 2016, BRATS 2017, BRATS 2018, BRATS 2019, BRATS, 2020 and recently the BRATS 2021. And some other lesser used datasets are: Figshare, LGG brain tumour segmentation, HBTR (Harvard Brain Tumour Repository), IRMA etc.

1. BRATS 2021: This dataset is defined as a collection of mpMRI scans of brain tumours that were gathered by various institutions. The original volumes are T1, T1-W, T1Gd (Gadolinium), T2-W (T2), and T2 Fluid Attenuated Inversion Recovery (T2-FLAIR) from the mpMRI scans are included in the BRATS 2021 challenge. These volumes were obtained using different methods and scanners from different institutions. Since then, the 2020 BRATS dataset cases 660 to 2000 have been used to update these data. Testing, validation, and training phases of the BRATS 2021 challenge had been separated. [27,28]
2. BRATS (2020): The EMA (Expectation Maximization Attention) configuration is used to retrieve so many significant aspects while removing duplicated data. The DSC and HD percentages of the total tumour are 91.1 and 4.13 percent, in both. The encoder-decoder segmented data method could indeed merge highly-resolved and low-resolution data and recognise characteristics at various scales; However, the short-term linkage between the encoding and decoding processes is obviously insufficient [29,30].
3. BRATS: 2018 BraTS collection contains 3D MRI scans from 285 people with brain tumours. This study comprised 210 individuals with malignant high grade glioma (HGG) and 75 patients with benign low grade gliomas (LGG). As of 2018, Bakas et al. a slow-growing tumour is LGG. The average lifespan of patients with this disease is often higher than 2 years. The tumour type HGG, on the other hand, develops rapidly. Usually, patients with tumours in the HGG group have less than two years to live. This population needs quick medical intervention if they have HGG tumours [32,90].
4. Figshare: Cheng devised the concept throughout 2017. The database contains 3064 MRI's brain's slices from 233 people. Brain tumours are classified into 3 categories: meningeal, hypophysis, and glioblastoma. The 762 is a phone number that can be used in signal processing circuitry as an example of signal processing. Meningioma necessitates 708 images, pituitary necessitates 930, and glioma necessitates 1426. (slices). On the Figshare website, the data set is available in MATLAB ".mat" format. A client ID, a distinctive label indicating this same sort of brain tumour, image information in 512*512 in uint16 configuration, a scalar chosen to represent the tumour cell bounds involved in a specific coordinate values, and support vectors in bitwise input images are all contained in each MAT-file [96].
5. BRATS 2017: Using MRI to visualize (display) tissue of brain is a very effective method. T1 and T2 MRI system configurations are two different types of MRI systems. T1-CE and T2-CE are both T1 and T2 imaging technique agreement enhancements. Other altered modalities that are frequently used are Flair's and Concentration Positron. We were using 4 distinct datasets for this study, which each is including graphic methodologies: IXI dataset [control subjects contain 582, three-dimensional objects (256 *256*140), MRI quantities from normal, IXI dataset [healthy subjects contain 582, three dimensional objects (256 *256*140), MRI editions from standard, IXI dataset [control subjects contain 582, three-dimensional objects (256 *256*140), MRI volumes from normal, Cheng datasets include 3064 two-dimensional (512 512) MRI images of three different diseases: meningial, glioblastoma, astrocytoma, and hypophysis. 230 2D (256 256) MRI images of three tumour types were provided by Hazrat-e-Rasool General Hospital [35].
6. BRATS 2016: The MRI techniques employed in this work included fluid attenuation inversion recovery, spin lattice relaxation-T1, spin lattice relaxation-T2, and spin-lattice relaxation contrast, or spin lattice relaxation-T2 (FLAIR). 230 brain scans make up the data, which also includes the centre pixel of the patch and 448,000 volume 32*32 modifications that were randomly selected. Thus, 448,000 patches and labels provide the training data for the suggested DCNN (Deep Convolutional neural networks). A batch size of 256 will result in 1750 iterations each epoch [36].
7. BRATS 2015: The "Central nervous system Tumour fragmentation" contest is globally known for its available to the public set of data, which is particularly used for checking developers' fragmentation algorithm. The term "Brain Cancer fragmentation" is an abbreviation for "Brain Tumour Segmentation." It includes 274 directories underneath the HGG and LGG categories, which each includes 5 MRI's images of brain tumours, MRI sequences namely Flair, T1, T1c, T2 and OOT are indeed the tumour kinds. For this reason, we were using Fluid Attenuated Reversal Retrieval (Flair) and Transverse Relaxation's duration's (T2) image's [37].
8. BRATS 2013: A brain tumour fragmentation dataset for the 2013 BRATS competition is composed of organic and real images that are further divided into HG and LG gliomas, respectively. Twenty instances have true HG photos, ten cases have real LG image data, and there are 25 patients who actually have both synthetic HG and LG images. For each patient's instance, MRI sequences and post-Gadolinium T1 magnetic resonance pictures are available [38].
9. BRATS 2012: The imputed sets of data which includes T1-w post-contrast and T2w central nervous system MRI images from 550 patients with validated and undiagnosed tumour's (female's 246 or male's 304). These same patients ranged in age from 15 versus 74 year's (mean age 48 year's). The images were obtained from a 1.5T MRI medical scanning at Shirdi Sai Cancer Hospital in Manipal, India, between February 2008 and March 2011. Each slice in the set of 64 obtained from each patient's scan had a thickness of 2 mm. The data collection contained only grayscale images, each measuring 640 x 480 pixels with a pixel size of 0.11 mm 0.11 mm. Sizes of the tumours ranged from 4 to 41 millimetres (mean size 21 mm). Out of 550

patients, 280 cases were treated for benign tumours and 270 patients' data were found to have malignant tumours based on histological analysis of biopsy samples. T1-w and T2w MRI images have been used in the experiments because they provide crucial diagnostics and make a clear differentiation between edoema and tumour cells [39].

10. MICAI (BRATS): Brain tumour MRI scans are part of the publicly accessible collection. The training set data contains 259 cases of extremely high gliomas (HG-High Grade) and 76 cases of low-grade gliomas (LGG). In the testing dataset, there are 125 samples. Within the training dataset and the images used to calculate the regression coefficients, T1, T1ce, T2, and FLAIR seem to represent the four multisensory image data. Glioblastoma (GBM/HGG) and gliomas of lower quality: preoperative multimodal MRI imaging (LGG). Multi-institutional standard clinically acquired, readily accessible OS, and pathologically verified diagnoses are offered as trained, validated, and tested data. In a 2017 study by Bakas, Akbari, Sotiras, et al [32, 40].
11. LGG-Brain tumour segmentation: Manual This dataset comprises brain MRI images with FLAIR aberrant segmentation masks. The photos are a part of the creation of the (TCIA) Cancer Imaging Archive. For at least 110 of the patients in the Cancer Genome Atlas (TCGA) LGG dataset, FLAIR-Fluid attenuated asymmetry recovery (healing) clump data were avail-able. [33].
12. HBTR (Harvard Brain Tumour Repository): The Harvard tumour repository was used in the second set of experiments, which included numerous stick shift specialist segmented results on two dimensional slices with 10 tumours. Due to its online availability, the characterized methods were used to analyze the efficiency of the various algorithms. T1w MRI images obtained the with SPGR series at 0.9375 *0.9375* 1.5 mm contiguous sagittal slices are used for the repository contrast images. This repository's data, known as STAPLE (Warfield, Zou & Wells, 2004), was recently evaluated using a validation framework for comparing the proposed approach to several specialist segmentation, which determines specificity, clarity, and total correct percent criteria. Using Harvard brain repository data, it is able to match inter - and intra variability versus computation reliability. [41].
13. IRMA: IRMA -Image Retrieval in Medical Applications is indeed a fully accessible set of data containing 12,677 unidentifiable CT images and 10,000 analyzed Image data in 193 and 57 classifications, respectively. Choose images from the 57-category labeled CT images for recovery experimentations. There are more than 100 graphics divided into 17 categories [42], and the number of different image's subgroups is fairly diverse. For experiments, photographs were chosen from these 17 categories, and for categories with fewer than 200 images, all images were chosen. A total of 200 photographs were chosen at random from each category for a total of more than 200 images. There were a total of 3,109 images chosen. Then, in a 4:1 ratio, divide the training and test sets.

The comparison of all the above mentioned datasets are summarized in Table 3.

6 Evaluation Metrics

To objectively assess the quality of segmentation techniques, various tumour kinds are first divided into three regions that are reciprocally exclusive:

1. the entire tumour (including several tumour's frameworks);
2. the centre of the tumour (excluding edema) and
3. a tumour that is currently growing in size (the "enhancing core").

The Dice score, Sensitivity, and Specificity are a few of the metrics used to gauge the algo- rithm's performance in each region. A research project must assess how well a machine learning system performs segmentation and classification. When only one metric, such as average ac- curacies scored, is employed, a machine learning model may yield results that are good when compared to other metrics, such as precision or any other measure. As a result, many differ- ent assessment criteria are routinely employed to evaluate and compare the performance of the model [43]. In a segmentation task, true positive (TP) pixels are those that are correctly pro- jected to belong to a particular class based on the underlying data, whereas true negative (TN) pixels are and those who are classed as not people who belong to a specified class. When the model incorrectly associates dots (or pixels) with a class when they do not, it produces a false positive (FP). Whenever the theory predicts this same category of a pixel inaccurately, a false negative (FN) occurs. TP denotes a tumored category that's also objective assurance to pertain to a specific class predicated just on actual truth, so although TN denotes a tumour category that's also reliably classified as being not belonging towards the specific class. A false positive (FP) is a result in which a cancer cell class that does not exist is fully realised. A FN occurs when the prototype predicts the member status of a class incorrectly. As a consequence, the fol- lowing paragraphs describe numerous performance measures used in the literary works on brain tumour cells automatic segmentation. The dice similarity coefficient (DSC) is used to evaluate the overlap of spatial between the segmented model region and the tumour region ground truth. The annotated model findings and the tumour region of the ground truth exhibit no spatial overlap, according to the DSC value of 0, where a value denotes total overlap. Mathematically, it is evaluated as:

$$DSC = \frac{2TP}{2TP + FN + FP} \quad (1)$$

A Hex score adjusts the true positive rate to match the size distribution of two structures of data. It is the same as the F-score (the harmonic mean of a highly precise recollect contour) and it can be monotonically changed to a Jaccard's score. Accuracy (ACC) is a statistic that evaluates a model's proficiency in classifying all possible courses or pixel densities, positive or negative.

$$ACC = \frac{TP + TN}{FP + FN + TP + TN}. \quad (2)$$

The sensitivity is the proportion of favourable predictions that are accurate when genuine positive samples or samples are randomly selected. It is determined whether the model can identify positive samples or pixels.

$$Sensitivity = \frac{TP}{FP + TP}. \quad (3)$$

Specificity which is denoted by SPE is the proportion of actual negatives that are portrayed as negative. It represents the proportion of pixels and courses that could not be identified.

$$SPE = \frac{TN}{TN + FP}. \quad (4)$$

Recall (RE) refers to the comprehensiveness of a ML model's true +ve predictions in relation towards the actual truth. It shows how many classes/pixels from our ground truth are used in the model's analysis.

$$RE = \frac{TP}{TP + FN}. \quad (5)$$

Precision which is denoted by PR, as well widely recognized as positive predictive value (PPV), is a statistical term that refers to a model's ability to predict. It shows how well the models predicted the proportion of positives.

$$PR = \frac{TP}{TP + FP}. \quad (6)$$

The most used metric for incorporating recall and precision is probably the same F1-Score. It stands for the harmonic mean of the two.

$$F1 = \frac{2 * PR * RE}{PR + RE}. \quad (7)$$

The Correlation indicator, commonly known as the intersection over union (IOU), calculates the percentage of overlapping between both the output of the model's prediction and the footnoted regression coefficients mask.

$$IOU = \frac{TP}{TP + FP + FN}. \quad (8)$$

7 Computer Aided Segmentation of brain tumour from MRI images

BTS methods take an MRI image as input, pre-process it for improving its quality and finally segment the brain tumour from the whole image. This section presents the detailed summary of pre-processing techniques and BTS methods used in the literature.

Table 4: Comparison of pre-processing techniques (Part 1)

Pre-processing Techniques	Meaning	Applications	References
N4ITK	It is a method for reducing non-uniformity and low frequency intensity in MRI images (bias/gain field).	This has been used to rectify flat fields in microscopic data.	[59]
Image Registration	The overlapping of two (or more) photographs for the purpose of detecting changes, identifying targets, or medical diagnosis is known as image registration. The alteration of an image's histogram to fit a defined histogram is known as histogram matching or histogram specification.	It is used to combine medical images, satellite images, and the purpose of detecting other types of images.	[45]
Histogram Matching	The alteration of an image's histogram to fit a defined histogram is known as histogram matching or histogram specification.	The goal of histogram matching is to take an image as input and generate an image based on the shape of a specified (or reference) histogram.	[46]
Normalization	MRI images are captured under different conditions, parameters. This degrades the performance of the MRI analysis methods. Thus, normalization techniques help to enhance the performance by reducing the parametric variations in the images.	The purpose of normalization is to make the database design more efficient.	[47, 91]
Noise Removal	Noise removal minimizes and wideband signal noise reduction algorithms	The visibility of noise is reduced or eliminated using noise reduction algorithms	[49]
Image Enhancement	The technique of increasing the quality and information to images to interpret and compare.	Enhancements are applied to images to make it easier to interpret and compare. processing is known as image enhancement.	[50]
Bias Field Correction	A predilection field signal is a reduced frequency, of tissue gain variation are extremely used by BFC to calculate a which contaminates Mri's correction field for the brain images data, particularly those produced by old MRI machines.	A series of local estimates of tissue gain variation are extremely seamless signal used by BFC to calculate a which contaminates Mri's correction field for the brain images data, particularly those produced by old MRI machines.	[51]

Table 5: Comparison of pre-processing techniques (Part 2)

Pre-processing Techniques	Meaning	Applications	References
Patch-based Intensity Normalization	Intensity normalization between images collected with different scanners or pulse sequences using patch-based normalization model.	An essential stage in the analysis of MRI brain pictures of the central nervous system is patch-based intensity normalization.	[52]
Augmentation	The process of modifying your data to produce several representations of the same samples is referred to as "augmentation" (usually to prevent overfitting).	The procedure of changing images to produce more representations of the same information is known as "augmentation" (usually to prevent overfitting).	[53]
Skull Stripping	Skull dissection is one of the steps in identifying brain issues.	In a brain MRI scan, it is initial process for differentiating brain tissue from other tissues.	[54]
Subsampling	By picking a subset of the data, subsampling minimizes data size.	Subsampling reduces the dependency on accurate localization inside feature maps generated by CNN convolutional layers.	[55]
Downsampling	When transmitting over limited bandwidth or when the spatial resolution is reduced while the two-dimensional (2D) representation remains the same.	Downsampling occurs a converting to a strained audio format, two-dimensional (2D) representation is used to reduce the bit rate.	[56]
Wavelets	A wavelet is just a mathematical operation that divides a continuous-time signal into distinct control applications, and the scale components.	The list of wavelet applications includes numerical or function analysis, signal analysis, and the analysis and adjusting of audio signals.	[57]

7.1 Pre-processing

The pre-processing approach improves the quality images of the brain tumour MRI images to make these suitable for further analysis. It also contributes to the enhancement of MRI image properties. Increased sensor ratio, better visual presence of MRI images data, expulsion of in- consequential loud sounds and back story of unwanted portions, attempting to smooth inner part areas, and maintaining relevant edges are some of the requirements [58] for better analysis. Following are the some techniques of pre-processing that are selectively applied to the MRI images:

N4ITK N4 is a bias field algorithm which corrects bias field and gain field in MRI imaging data. It is a method for reducing non-uniformity and low frequency intensity in MRI images (bias/gain field). An adaptation of the well-known N3 technique for non-parametric non-uniform intensity normalisation is suggested for bias field correction [59].

Bias Field Correction (BFC) A predilection field signal is a reduced frequency, extremely seamless signal which contaminates MRI's images data, particularly those produced by old MRI machines. Using a number of local estimations of tissue gain variation, BFC determines a correction field for the brain region [51].

Patch based Intensity Normalization A patch-based generative model is used to normalise the intensity of images taken with various scanners or pulse sequence settings. In the analysis of MRI brain images of the central nervous system, patch-based intensity normalisation is a crucial pre-processing step [52].

Image Registration In order to assure the spatial correspondence of anatomy across numerous images, multiple images are aligned using a technique called image registration [45]. It is an important technique in many biomedical imaging systems. These overlaid images enhance the visibility of different and common features that are extremely significant for tumour detection.

Histogram Matching It is an easy way for matching one image to the next in terms of calibration. Histogram matching, also known as histogram specification, is the change of images histogram to meet a specified histogram. The purpose of histogram matching is to take a image as input and create an image based on the design of a predetermined (or reference) histogram [46].

Normalization MRI images are captured under different conditions, devices and parameters. This degrades the performance of the MRI analysis methods. Thus, normalization techniques help to enhance the performance by reducing the parametric variations in the images [47]. Normalization have some most commonly used techniques like contrast stretching, Z-score normalization etc. Contrast Stretching is an part of the normalization. An image's dynamic range, or the "spread" of its histogram, is measured by its contrast. Pictures with weak contrast owing to glare, etc [91]. Intensity normalisation is a crucial step in the MRI preparation process when segmenting data using classification and clustering methods. Because of confounding effects caused by changes in brain tumour shape, segmenting cancer images is much more difficult than fragmenting healthy images. A pathology-resistant normalization method for MRI images was presented in order to improve both global and local limitations. To reduce the effect of magnetic field non - uniformity all through images acquired, a bias-field correction was applied prior to the segmentation method.

Once pre-processing the multimodal images data, all methodologies must be registered in a single reference space. A linear new identity with Mutual Information (MI) similarity measure and resampling are typically used to ensure voxel-to-voxel connection throughout all methodologies. The brain's preliminary processing MRI scans are essential for better outcomes. Many machine learning approaches can benefit from the pre-processing phase known as Z-score normalisation. Rescaling the features to give them the properties of a standard normal distribution—that is, an average of zero and an SD of just one is what standardisation requires. A pre-processing procedure called Z-score normalisation can help a lot of machine learning methods. Standardization includes scaling the characteristics to have only a zero average and a single standard deviation (SD), as in a typical normal distribution. The Z-score, a kind of scale, shows how many standard deviations there are from the mean. Z-score can be used to determine if the mean is 0 and standard deviation is 1 of your feature distributions. It is helpful when there are a few outliers but not enough that pruning is required [47].

Noise removal Noise removal minimizes back-ground and wide-band noise while preserving signal quality. Noise reduction methods reduce or completely remove the appearance of disturbance by averaging overall entire image and preserving regions near intensity boundary lines [49].

Image Enhancement The technique of increasing the quality and information content of raw data before processing is known as image enhancement. Enhancements are applied to images to make it easier to interpret and comprehend [50].

Augmentation The technique of altering images to produce several representations of the same information is known as image augmentation. The term "augmentation" refers to the process of modifying your data in order to generate more samples (usually to prevent overfitting) [53].

Skull stripping Due to the complexity of the human brain, the wide range of MRI scanner parameters, and individual features, the process of skull stripping is challenging. Poor-quality and low-contrast images make accurate segmentation even more difficult. Several powerful skull stripping treatments have been developed to remove these impacts. The removal of the skull is one of the initial steps in identifying brain issues. It is the process used to distinguish brain tissue by other tissues during a MRI scan of the brain. [54].

Sub sampling By picking a subset of the original data, subsampling minimizes data size. Subsampling reduces the dependency on accurate location inside feature maps generated by CNN convolutional layers [55].

Down Sampling MRI images are of super resolution. Several machine learning and deep learning methods have achieved better and fast results using lesser resolution images i.e. down sampling the images. Down sampling occurs when the spatial resolution is reduced while the two-dimensional (2D) representation remains the same [56].

Wavelets A wavelet is just a mathematical operation that divides a continuous-time signal or function into distinct scale components. The list of wavelet applications includes numerical analysis, signal analysis, control applications, and the analysis and adjusting of audio signals [57].

All the pre-processing techniques are summarized in Tables 4 and 5.

7.2 Segmentation

After pre-processing, brain tumour is extracted from the pre-processed MRI images. BTS methods are classified into three primary classes: traditional methods, machine learning (ML) based methods and deep Learning based methods [60] (see Figure 2).

Traditional methods for brain tumour segmentation Traditional segmentation techniques are broken down into four groups based on different concepts and wording: Threshold, region, fuzzy-theory, and edge detection-based traditional (conventional) segmentation approaches [61].

1. **Thresholding:** Thresholding is the oldest technique which is used for the image segmentation methods. Threshold-based segmentation is the easiest technique. To begin, all pixels within a range are assumed to be of the same type [60]. Setting an adequate threshold divides brain tumour images into target and background regions. An improved threshold segmentation approach Using local information from pixel neighbours, the method enhances noise sensitivity in threshold segmentation [62,63]. The image is expected to be made up of regions that belong to distinct grey scale of scale ranges during the thresholding procedure. The highs and lows in the image histogram are made up of peaks that each indicate a different region. The dips between the peaks here signify a threshold value. The threshold-based segmentation approach is straightforward, but choosing the appropriate threshold is crucial because the value of a segmented resultant is almost entirely influenced by threshold size. Additionally, the threshold segmentation technique was limited to simple picture segmentation, making it challenging to handle increasingly complex images.
2. **Region-based segmentation** We employ connection to keep distinct elements of the image from being connected. To begin, we must first specify the seeding of the pixel. We could designate every pixel as seeding the pixels or selecting pixels randomly. Extend regions till they contain all of the image pixels. The Watershed algorithm and the Region-growing algorithm are two popular region-based segmentation algorithms. The Watershed algorithm is a set of numerical morphological features used in segmentation. The images to be filtered are evaluated to topographical in geographic location in this procedure, with the grey benefit of the pixels defining the height of the scene. The term "ponding basin" refers to the neighbourhood minimum and its surroundings. For every relatively minimum, it is assumed that highly porous pores exist. The standing water basin would then progressively be flooded

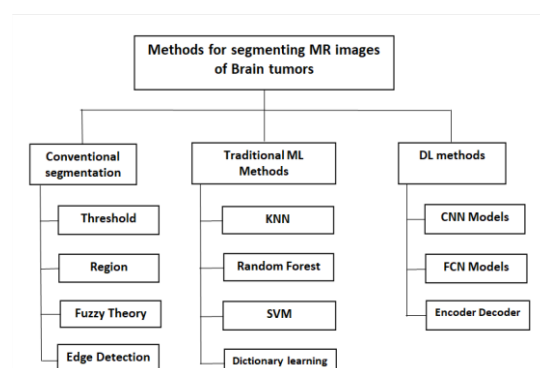


Fig. 2: Methods for segmenting MRI images of brain tumours

as the level of penetration water rises. A dam is a structure that blocks the flow of water from one body of water to another. The infiltration process is complete whenever the level of water reaches its highest point. These dams are referred to as watersheds. A group of people who work together to solve problems [64]. An innovative method that combines watershed and threshold segmentation [65]. The image was initially divided into segments using the threshold approach, and then the watershed algorithm was used to divide the segments. The experiments showed that the segmented findings obtained using this method had a TPR (temperature, pulse, respiration) of above 90%, making them more reliable than any obtained using either of the two techniques alone. A straightforward technique for segmenting a picture based on regions is known as "region expanding." It is categorised as a pixel-based technique because it requires the first seed point selection. It's better than the edge based segmentation techniques because in noisy images it is difficult to detect the edges for the segmentation. The area-based edge detection technique has the advantages of becoming easy and accurate, allowing for more regional information extraction and making it ideal for segmenting small objects. It is, however, a subtle sound that easily creates gaps in harvested areas.

3. **Fuzzy Theory** Segmented algorithms based on fuzzy theory are also well-liked. According to LEI, ZHANG, JIA, LIU, and ZHANG [66, 67], fuzzy C-means (FCM) clustering is the approach that uses fuzzy theory that is most frequently used in brain tumour MRI image segmentation (Muneer & Joseph, 2018). The K FCM technique was created by combining the FCM and K - means algorithms. The investigation showed that K-FCM segmented brain tumour MRI images more accurately and with less computational complexity than FCM [68].
4. **Edge Detection-Based Segmentation Methods** A technique called edge detection identifies the edges of the objects in the photos. It detects the discontinuities in brightness. It segmented the images and retrieved data in image processing segmentation and data extraction. The target curve segmentation principle works by first acquiring the target region's edge and then acquiring the target region's contour. The Roberts, Sobel, Canny, but also Prewitt edge detection operators are all widely used [69, 70]. The active contour model now has FCM built in. FCM chooses the model's initial shape for you, reducing the amount of time you have to communicate with the computer. Furthermore, the issue of MRI images with an unsure border contour and inconsistent intensity has been resolved.

Machine Learning based methods for brain tumour segmentation According to conventional machine learning techniques, this same categorised model is trained using predefined criteria for brain tumour segmentation (BTS) procedures. They are typically divided into two categories: organizational and sensor. The classifier must determine which form of organization so every functionality belongs to at the organizational level, as well as which category so every data point is classified as belonging to at the pixel level. A popular machine learning method is K-Nearest Neighbors (KNN) [71], Support Vector Machine (SVM) [72], Random Forest (RF) [73], Dictionary Learning [74].

1. **KNN** The KNN method was used to segment each brain as though it were a separate database. They got highly accurate findings, and each brain picture segmentation took only one minute, which improved segmentation efficiency [72].
2. **SVM** For the image segmentation, SVM is proposed. It can reduce the segmentation errors caused by quick motion of the objects. SVM was used to fragment brain cancers, keeping into consideration the changing attributes on signal strength as well as other MRI image parameters. After that, features have been extracted using wavelet transform transformation,

Table 6: Comparison of segmentation techniques (Part 1)

Segmentation Techniques	Description	Advantages	Limitations	References
Threshold segmentation	Seg- Thresholding is a method for segmenting the images in which all of the pixels within a range are first presumptively of the same kind. A colour or grayscale image is transformed into a binary image (black and white) by this procedure.	Being simpler to calculate, and As you start reducing de- tails to something like a binary variable, thresholding invariably throws out data that you'll never be willing to use again.		[60,62,63]
Region Segmentation	The technique of determining the regions directly is known as the main goal is to divide an image into different regions.	Could really properly distinguish between regions with the and sensitive to noise.region based segmentation. The same properties which we de-	It is time consuming to compute	[64,65,112]
Fuzzy Theory	Fuzzy based segmentation, These systems are dependable and handle a range of inputs the results they are not usually and region based features of the without needing precise input.image, which merge the regions recursively.	Because of the unreliability of [64,65,68,113,114]which combines the both edge and can	universally recognised.	[64,65,68,113,114]
Edge Detection	This approach for detecting detection is used for seamless transition images is ages.	It recognises different brightness Noise segmentation and data extraction and computer vision.	Noise sensitivity, Working on [69, 70, 115, 116]edges of the items among im- levels. Edge proving to be difficult.in fields like image process-	[69, 70, 115, 116]
KNN	KNN searches for similar characteristics that are comparable to those of its nearest neighbours.	It is used for the real time pre-determining the right value of "k" is challenging.		[117]
SVM	Both classification and regression. It's used it does not perform well because it.	In high dimensional spaces, When we have a large dataset, [118]ion issues can be solved using SVM is more effective. It needed a training time longer.		[118]

Table 7: Comparison of segmentation techniques (Part 2)

Segmentation Techniques	Description	Advantages	Limitations	References
Random forest	Both classification and regression employ this approach for a variety of graphic elements performs poorly on data that is decision trees.	They have the capacity to handle a variety of graphic elements with ease for both classification and regression, and they are computationally efficient.	One of its major flaws is that it performs poorly on data that is un-balanced and regression, and they are computationally inefficient.	[119]
Dictionary Learning	It is a form of machine learning and signal processing. It found a frame called Dictionary. It is represented sparsely in some training data, and sparse representation is better.	It is used to analyse the medical and signal processing. It found signals.		[74]
CNN	In pattern recognition and object identification, CNN is often used for segmenting the images, ages, having a better contrast solving complex problems.	It gives the most precise find- It's needed for the large training data. Images with different positions are classified. and this approach is used for between objects.		[101]
FCN	FCN is a semantic segmentation which consists of the encoding part for the feature extraction. It segments the boundaries layers that means the fewer parameters that can make the net-work faster.	It is avoided to use the dense layers that means the fewer parameters that can make the net-work faster.		[120], [121]
Encoder-decoder	It is typically found in an encoder-decoder configuration. Encoder structure is frequently used for segmentation. It is derived primarily from core classification networks like VGG, etc.	Compactable in sizes, high resolution. Which is training the images distinctive feature map. Encoder structure is frequently used for segmentation. It is derived primarily from core classification networks like VGG, etc.	The size must be comparable with the actual sizes always because it uses many encoders and decoders.	[122], [123]

and the functionality component was whittled down using Principal component analysis to obtain the best characteristics for SVM (support vector machine) clustering [75]. Brain developed an approach in which the picture is initially segmented into super-voxels, the tumour is segmented using MRF, the likelihood function is estimated simultaneously, and a multistage wavelet filter is used to extract the features. It is suggested a texture and contour based automatic segmentation technique [76]. By specifying the grayscale and texture information in various areas of the image, one such approach can quickly and accurately segment an image. When utilised to segment the brain tumour MRI images, the usual machine learning approach performs worse than a variety of conventional segmentation algorithms in terms of algorithmic performance. For instance, the K-nearest Neighbour approach can locate tumours in the central nervous system with good accuracy and ease of implementation, although it is computationally intensive. The final conclusion is decided by a huge number of support vectors, and the svm classifier does have a strong hypothesis. Although the algorithm is simple and has good generalizability, the parameters and kernel function selection criteria are more demanding. High anti-noise performance and effective over-segmentation handling are two strengths of random forest. It can speed up operations by paralleling them, but it's not very good at processing low-dimensional tumour data is easy to create and the learning-based technique is similar to a dimensionality reduction concept in that both reduce computing complexity and speed, because both have stricter standards for tumour data. The learning-based technique has a high prediction accuracy for brain tumour location, but it requires a lot of computation.

- 3. Random Forest:** It is utilised to separate the normal tissues from the various tumour portions in the MRI image voxels. Brain lesions are the type of damage in the brain due to the disease. Lesion segmentation is being done with the help of random forest classifiers. Segmenting lesions from images, such as those from MRI, ultrasound, or CT scans, entails categorising the pixels in the images into one or more classes. This for both classification and regression employ this approach for the decision trees. They have the capacity to handle a variety of the graphic elements with ease for both classification and regression and they are computationally efficient. one of the major flaws is that it performs poorly on data that is unbalanced [77, 78].
- 4. Dictionary Learning:** It is a classifier that uses an algorithm to categorise the data. If it turns out to be non-linear, supervised learning is applied to the data before the information is translated into linear form. Finally, dictionary learning is used for regularisation in the final layers. It is a form of machine learning and signal processing. It found a frame called Dictionary. It is represented sparsely in some training data, and sparse representation is better. It is used to analyse the medical data [79]

Deep Learning based methods for brain tumour segmentation The central nervous system MRI classification focus on solving on Deep Learning and thus it could be broken down into three types: CNN, Fully Convolutional Neural Network (FCN) Magnetic resonance image segmented method for neurological disorders, or even encoder and decoder based on different network frameworks.

1. Brain tumour segmentation using CNN

CNN is a weight-sharing technique. It is a type of neural network and significantly reduces the model's complexity. CNN could start with an image sequence, remove outliers instantaneously, and want to have a significant level of nonlinearities to transcription of images, scalability, as well as other changes. There have been numerous grid models based on CNNs developed in recent years (convolutional neural networks), such as Network [80], VGG [81], GoogleNet, Res-Net [82], etc. In medical image segmentation, they are commonly employed. To address the issue of network degradation, follow these steps. It merged a 3D deep neural network with closely packed connections, pretrained this same model, and used the weight gained to initialize the model [83]. This technique improved the DSC measure when segmenting brain tumour MRI images. It accumulates a double path CNN that uses the output character trait graph from the beginning stage as an additional input to the second stage's CNN. With the use of this technique, segmentation accuracy can be increased while collecting thorough background data. It's used by N4ITK to correct the bias field, multi classification CNN to pre-segment it, and median filtering to get the final segmentation results. For the diagnosis of brain tumour magnetic resonance imaging in particular, the rise in the DSCs recorded to 90% will have produced great results. The CNN-based segmentation method could indeed instantaneously remove the noise and handle close to the edge data, and yet information can be lost during the pooling process, and it is difficult to understand.

2. **Brain tumour segmentation using FCN** FCN performs better at semantic image segmentation. This same representation of the input image is unimportant to FCN, but the final convolutions layers will be upsampled. This method achieves the same effect as the input vector sized images by anticipating every data point whereas trying to retain this same sensory data in the source images. A method of segmenting and classifying images at the pixel level is FCN. As a result, the FCN-based linguistic segmented model is notably more in line with the specifications for medical picture interpretation. To fragment/segment brain tumours, they combine FCN and CRF. The process starts with segmenting images of brain tumours, followed by training 2D slices inside the axial, coronal, and sagittal views. The performance and segmentation rate are both higher when compared to more established segmentation techniques [83]. The most widely used brain tumour segmentation model is an FCN-based U-Net, in which the networks are designed to incorporate both an encoded and a decoded, A U-Net networks jump connections would code path, using its attributes of both the managed to figure out the decoding route to a corresponding point, in order to have the positive attributes of the prior findings under coding phase into the decoding process, and therefore start learning extra clear plans.

3. **Brain tumour segmentation Using Encoder-Decoder** An encoder and a decoder are typically found in the encoders-decoders configuration. In addition to obtaining the image's distinctive feature map, an encoder uses neural networks to train and gain knowledge of it as input. After the encoder has supplied a feature map that produces the edge detection effect, the decoder's responsibility is to specify the category of each pixel. Encoder structure is frequently comparable in object segmentation premised on encoder decoder framework, which is derived primarily from core classification networks like VGG, etc. The objective is to use a large database to train network weight parameters. As a result, the decoder's difference reflects the network's difference to a large measure, which is a major determinant of the categorization impact. This framework is more advanced than others in terms of context pixel segmentation and outperforms them. Learning the characteristics of sparsely annotated volume images with a three-dimensional U-Net approach. It built an HDC (Hybrid Dilated Convolution) module on top of the 3D U-Net to expand neurons' sensory fields, bypassing the limitation imposed by DCN's non-linear and non extracting features. The amount of design variables and computational time can be cut in half through using superficial neural network models. The DSC, TPR, and PPV measures are managed to improve so over traditional U-Net structure, using a layered depth cross-modal convolution of cross mode shape encoder/decoder framework in mixture with MRI image data from multiple methodologies, and also normalized and number of stages training techniques to fix the issue of outliers [124–126]. All the preprocessing techniques are summarized in Tables 6 and 7.

8 Conclusions

This study provides comprehensive insights into recent advancements in MRI-based brain tumour segmentation methods, aiming to establish a strong foundation for researchers interested in developing such methods. Beginning with an overview of brain anatomy, followed by a discussion on imaging modalities, this work sets the stage for understanding the complexities of brain tumour segmentation from MRI images. Various datasets utilized for brain tumour segmentation from 2012 to 2021 were reviewed, with the BRATS dataset emerging as the most widely used in the literature. Performance evaluation of segmentation methods is commonly conducted using metrics such as dice score, sensitivity, specificity, and accuracy. Numerous algorithms, including convolutional, traditional, and deep learning methods, are employed for brain tumour classification and segmentation. Recent advancements have seen the proposal of new deep learning and machine learning algorithms for research purposes. Future research is expected to focus on developing computational segmentation techniques that are faster and more accurate. This may involve exploring novel preprocessing techniques, such as noise removal, histogram matching, and normalization methods, to enhance

the segmentation process.

While significant progress has been made in developing systems based on deep learning and image processing for tumour segmentation, there remains a need to analyze contextualized functionality during feature extraction and to explore the creation of new features. Magnetic resonance-based tumour segmentation techniques have already demonstrated promising results in clinical practice, and further advancements in this area are anticipated to yield even better outcomes in tumour detection and analysis.

Declarations

Funding: No funding received for this research.

Data Availability: The dataset generated and analyzed during the current study is available from the corresponding author on reasonable request.

Conflict of interest: No conflict of interest.

References

1. Gordillo, Nelly, Montseny, Eduard, Sobrevilla and Pilar, "State of the art survey on MRI brain tumor segmentation," in Magnetic resonance imaging, vol. 31, pp. 1426–1438, 2013.
2. Gupta, Ms Pritee and Shringirishi, Ms Mrinalini and others, "Implementation of brain tumor segmentation in brain mr images using k-means clustering and fuzzy c-means algorithm," in International Journal of Computers & Technology, vol. 5, pp. 54–59, 2013.
3. Bondy, Melissa L and Scheurer, Michael E and Malmer, Beatrice and Barnholtz-Sloan, Jill S and Davis, Faith G and Il'Yasova, Dora and Kruchko, Carol and McCarthy, Bridget J and Rajaraman, Preetha and Schwartzbaum, Judith A and others, "Brain tumor epidemiology: consensus from the Brain Tumor Epidemiology Consortium," in Cancer, vol. 113, pp. 1953–1968, 2008.
4. Sharma, Preeti and Shukla, Anand Prakash, "A Review on Brain Tumor Segmentation and Classification for MRI Images," in 2021 International Conference on Advance Computing and Innovative Technologies in Engineering (ICACITE), pp. 963–967, 2021.
5. Hoffman, Edward J and Huang, Sung-Cheng and Phelps, Michael E, "Quantitation in positron emission computed tomography: 1. Effect of object size.," in Journal of computer assisted tomography, vol. 3, pp. 299–308, 1979.
6. Hounsfield, Godfrey N, "Computerized transverse axial scanning (tomography): Part 1. Description of system," in The British journal of radiology, vol. 46, pp. 1016–1022, 1973.
7. Amiri, S., Rezik, I. and Mahjoub, M. A. (2016). Deep random forest-based learning transfer to svm for brain tumor segmentation, 2016 2nd International Conference on advanced technologies for signal and image processing (ATSIP), IEEE, pp. 297–302.
8. Arakeri, M. P. and Reddy, G. R. M. (2015). Computer-aided diagnosis system for tissue characterization of brain tumor on magnetic resonance images, Signal, Image and Video Processing 9(2): 409–425.
9. Archa, S. and Kumar, C. S. (2018). Segmentation of brain tumor in mri images using cnn with edge detection, 2018 International Conference on Emerging Trends and Innovations in Engineering and Technological Research (ICETIETR), IEEE, pp. 1–4.
10. M. F. M. Lima and J. A. T. Machado, "Towards a classification scheme for musical sounds," 2013 Signal Processing: Algorithms, Architectures, Arrangements, and Applications (SPA), 2013, pp. 195–199. This paper analyzes musical opus of different musical styles.
11. Archip, N., Jolesz, F. A. and Warfield, S. K. (2007). A validation framework for brain tumor segmentation, Academic radiology 14(10): 1242–1251.
12. Aslam, A., Khan, E. and Beg, M. S. (2015). Improved edge detection algorithm for brain tumor segmentation, Procedia Computer Science 58: 430–437.
13. Baid, U., Ghodasara, S., Mohan, S., Bilello, M., Calabrese, E., Colak, E., Farahani, K., Kalpathy-Cramer, J., Kitamura, F. C., Pati, S. et al. (2021). The rsna-asnr-miccai brats 2021 benchmark on brain tumor segmentation and radiogenomic classification, arXiv preprint arXiv:2107.02314.
14. Bakas, S., Akbari, H., Sotiras, A. et al. (2017). Segmentation labels for the pre-operative scans of the tcga-gbm collection. the cancer imaging archive.
15. Bakas, S., Reyes, M., Jakab, A., Bauer, S., Rempfler, M., Crimi, A., Shinohara, R. T., Berger, C., Ha, S. M., Rozycki, M. et al. (2018). Identifying the best machine learning algorithms for brain tumor segmentation, progression assessment, and overall survival prediction in the brats challenge, arXiv preprint arXiv:1811.02629 .
16. Bal, A., Banerjee, M., Chaki, R. and Sharma, P. (2021). An efficient brain tumor image classifier by combining multi-pathway cascaded deep neural network and handcrafted features in mr images, Medical & Biological Engineering & Computing 59(7): 1495–1527.
17. Bashir-Gonbadi, F. and Khotanlou, H. (2021). Brain tumor classification using deep convolutional autoencoder-based neural network: multi-task approach, Multimedia Tools and Applications 80(13): 19909–19929.
18. Basser, P. J. and Jones, D. K. (2002). Diffusion-tensor mri: theory, experimental design and data analysis—a technical review, NMR in Biomedicine: An International Journal Devoted to the Development and Application of Magnetic Resonance In Vivo 15(7-8): 456–467.
19. Belliveau, J., Kennedy, D., McKinstry, R., Buchbinder, B., Weisskoff, R., Cohen, M., Vevea, J., Brady, T. and Rosen, B. (1991). Functional mapping of the human visual cortex by magnetic resonance imaging, Science 254(5032): 716–719.

20. Biratu, E. S., Schwenker, F., Ayano, Y. M. and Debelee, T. G. (2021). A survey of brain tumor segmentation and classification algorithms, *Journal of Imaging* 7(9): 179. Blezek, D. J. and Erickson, B. J. (1959). Lionel t. cheng, *Informatics in Medical Imaging* p. 219.
21. Buda, M., Saha, A. and Mazurowski, M. A. (2019). Association of genomic subtypes of lower- grade gliomas with shape features automatically extracted by a deep learning algorithm, *Com- puters in biology and medicine* 109: 218–225.
22. Bukhari, S. T. and Mohy-ud Din, H. (2021). E1d3 u-net for brain tumor segmentation: Submis- sion to the rsna-asnr-miccai brats 2021 challenge, arXiv preprint arXiv:2110.02519 .
23. Canny, J. (1986). A computational approach to edge detection, *IEEE Transactions on pattern analysis and machine intelligence* (6): 679–698.
24. Chen, X., Nguyen, B. P., Chui, C.-K. and Ong, S.-H. (2016). Automated brain tumor segmen- tation using kernel dictionary learning and superpixel-level features, 2016 IEEE International Conference on Systems, Man, and Cybernetics (SMC), IEEE, pp. 002547–002552.
25. Cheng, G., Cheng, J., Luo, M., He, L., Tian, Y. and Wang, R. (2020). Effective and efficient multitask learning for brain tumor segmentation, *Journal of Real-Time Image Processing* 17(6): 1951–1960.
26. Cheng, G. and Ji, H. (2020). Adversarial perturbation on mri modalities in brain tumor seg- mentation, *IEEE Access* 8: 206009–206015.
27. Chikhalikar, A. and Dharwadkar, N. (2021). Model for enhancement and segmentation of mag- netic resonance images for brain tumor classification, *Pattern Recognition and Image Analysis* 31(1): 49–59.
28. Choi, S.-G. and Sohn, C.-B. (2019). Detection of hgg and lgg brain tumors using u-net, *Medico Legal Update* 19(1): 560–565.
29. Ci cek, O., Abdulkadir, A., Lienkamp, S. S., Brox, T. and Ronneberger, O. (2016). 3d u-net: learning dense volumetric segmentation from sparse annotation, *International conference on medical image computing and computer-assisted intervention*, Springer, pp. 424–432.
30. Cui, B., Xie, M. and Wang, C. (2019). A deep convolutional neural network learning transfer to svm- based segmentation method for brain tumor, 2019 IEEE 11th International Conference on Advanced Infocomm Technology (ICAIT), IEEE, pp. 1–5.
31. Damadian, R., Zaner, K., Hor, D., DiMaio, T., Minkoff, L. and Goldsmith, M. (1973). Nuclear magnetic resonance as a new tool in cancer research: human tumors by nmr, *Annals of the New York Academy of Sciences* 222(1): 1048–1076.
32. Demirhan, A., Toru, M. and Guler, I. (2014). Segmentation of tumor and edema along with healthy tissues of brain using wavelets and neural networks, *IEEE journal of biomedical and health informatics* 19(4): 1451–1458.
33. Mateusz Buda, Ashirbani Saha, Maciej A. Mazurowski, Association of genomic subtypes of lower-grade gliomas with shape features automatically extracted by a deep learning algorithm, *Computers in Biology and Medicine*, Volume 109, 2019, Pages 218-225, ISSN 0010-4825
34. Detre, J. A., Rao, H., Wang, D. J., Chen, Y. F. and Wang, Z. (2012). Applications of arterial spin labeled mri in the brain, *Journal of Magnetic Resonance Imaging* 35(5): 1026–1037.
35. Di Ieva, A., Russo, C., Liu, S., Jian, A., Bai, M. Y., Qian, Y. and Magnussen, J. S. (2021). Application of deep learning for automatic segmentation of brain tumors on magnetic resonance imaging: a heuristic approach in the clinical scenario, *Neuroradiology* pp. 1–10.
36. Dou, W., Ruan, S., Chen, Y., Bloyet, D. and Constans, J.-M. (2007). A framework of fuzzy information fusion for the segmentation of brain tumor tissues on mr images, *Image and vision Computing* 25(2): 164–171.
37. Duong, H.-T. and Nguyen-Thi, T.-A. (2021). A review: preprocessing techniques and data aug- mentation for sentiment analysis, *Computational Social Networks* 8(1): 1–16.
38. Eijgelaar, E. and Peeters, P. (2020). Minder vliegen moet, maar hoe doen we dat?, *S&77*(1): 5–14.
39. Fooladivanda, A., Shokouhi, S. B., Ahmadinejad, N. and Mosavi, M. R. (2014). Automatic segmentation of breast and fibroglandular tissue in breast mri using local adaptive thresholding, 2014 21th Iranian Conference on Biomedical Engineering (ICBME), IEEE, pp. 195–200.
40. Ghosal, P., Nandanwar, L., Kanchan, S., Bhadra, A., Chakraborty, J. and Nandi, D. (2019). Brain tumor classification using resnet-101 based squeeze and excitation deep neural net- work, 2019 Second International Conference on Advanced Computational and Communication Paradigms (ICACCP), IEEE, pp. 1–6.
41. Guerquin-Kern, M., Haberlin, M., Pruessmann, K. P. and Unser, M. (2011). A fast wavelet-based reconstruction method for magnetic resonance imaging, *IEEE transactions on medical imaging* 30(9): 1649–1660.
42. Guo, Y. and Sengur, A. (2015). Ncm: Neutrosophic c-means clustering algorithm, *Pattern Recog- nition* 48(8): 2710–2724.
43. Gupta, M. P., Shringirishi, M. M. et al. (2013). Implementation of brain tumor segmentation in brain mr images using k-means clustering and fuzzy c-means algorithm, *International Journal of Computers Technology* 5(1): 54–59.
44. Havaei, M., Jodoin, P.-M. and Larochelle, H. (2014a). Efficient interactive brain tumor seg- mentation as within-brain knn classification, 2014 22nd international conference on pattern recognition, IEEE, pp. 556–561.
45. Havaei, M., Larochelle, H., Poulin, P. and Jodoin, P.-M. (2016). Within-brain classification for brain tumor segmentation, *International journal of computer assisted radiology and surgery* 11(5): 777–788.
46. He, K., Zhang, X., Ren, S. and Sun, J. (2016). Deep residual learning for image recognition, *Proceedings of the IEEE conference on computer vision and pattern recognition*, pp. 770–778.
47. Hoffman, E. J., Huang, S.-C. and Phelps, M. E. (1979). Quantitation in positron emission computed tomography: 1. effect of object size., *Journal of computer assisted tomography* 3(3):299–308.
48. Hoseini, F., Shahbahrami, A. and Bayat, P. (2018). An efficient implementation of deep convo- lutional neural networks for mri segmentation, *Journal of digital imaging* 31(5): 738–747.
49. Hounsfield, G. N. (1973). Computerized transverse axial scanning (tomography): Part 1. de- scription of system, *The British journal of radiology* 46(552): 1016–1022.
50. Huang, B., Xiao, H., Liu, W., Zhang, Y., Wu, H., Wang, W., Yang, Y., Yang, Y., Miller, G. W., Li, T. et al. (2021). Mri super- resolution via realistic downsampling with adversarial learning, *Physics in Medicine & Biology* 66(20): 205004.
51. Isensee, F., Jager, P. F., Full, P. M., Vollmuth, P. and Maier- Hein, K. H. (2020). nnu-net for brain tumor segmentation, *International MICCAI Brainlesion Workshop*, Springer, pp. 118–132.

52. Jayanthi, S., Ranganathan, H. and Palanivelan, M. (2019). Segmenting brain tumour regions with fuzzy integrated active contours, *IETE Journal of Research* pp. 1–12.
53. Juntu, J., Sijbers, J., Van Dyck, D. and Gielen, J. (2005). Bias field correction for mri images, *Computer recognition systems*, Springer, pp. 543–551.
54. Kalavathi, P. and Prasath, V. S. (2016). Methods on skull stripping of mri head scan images—a review, *Journal of digital imaging* 29(3): 365–379.
55. Kaleem, M., Sanaullah, M., Hussain, M. A., Jaffar, M. A. and Choi, T.-S. (2012). Segmentation of brain tumor tissue using marker controlled watershed transform method, *International MultiTopic Conference*, Springer, pp. 222–227.
56. Khan, S. A. R., Yu, Z., Belhadi, A. and Mardani, A. (2020). Investigating the effects of renewable energy on international trade and environmental quality, *Journal of Environmental management* 272: 111089.
57. Kleesiek, J., Biller, A., Urban, G., Kothe, U., Bendszus, M. and Hamprecht, F. (2014). Ilastik for multi-modal brain tumor segmentation, *Proceedings MICCAI BraTS (brain tumor segmentation challenge)* pp. 12–17.
58. Krizhevsky, A., Sutskever, I. and Hinton, G. E. (2012). Imagenet classification with deep convolutional neural networks, *Advances in neural information processing systems* 25: 1097–1105.
59. Kucharczyk, J., Mintorovitch, J., Asgari, H. S. and Moseley, M. (1991). Diffusion/perfusion mr imaging of acute cerebral ischemia, *Magnetic resonance in medicine* 19(2): 311–315.
60. Kumar, D. M., Satyanarayana, D. and Prasad, M. G. (2021). An improved gabor wavelet transform and rough k-means clustering algorithm for mri brain tumor image segmentation, *Multi-media Tools and Applications* 80(5): 6939–6957.
61. Kumar, S., Negi, A., Singh, J. and Verma, H. (2018). A deep learning for brain tumor mri images semantic segmentation using fcn, *2018 4th International Conference on Computing Communication and Automation (ICCCA)*, IEEE, pp. 1–4.
62. LEI, T., ZHANG, X., JIA, X.-h., LIU, S.-g. and ZHANG, Y.-n. (2019). Research progress on image segmentation based on fuzzy clustering, *ACTA ELECTRONICA SINICA* 47(8): 1776.
63. Liu, L., Feng, D., Chen, G., Chen, M., Zheng, Q., Song, P., Ma, Q., Zhu, C., Wang, R., Qi, W. et al. (2012). Mitochondrial outer-membrane protein fundc1 mediates hypoxia-induced mitophagy in mammalian cells, *Nature cell biology* 14(2): 177–185.
64. Lloyd, C. T., Sorichetta, A. and Tatem, A. J. (2017). High resolution global gridded data for use in population studies, *Scientific data* 4(1): 1–17.
65. Mahmood, Q. and Basit, A. (2015). Automatic ischemic stroke lesion segmentation in multi-spectral mri images using random forests classifier, *BrainLes 2015*, Springer, pp. 266–274.
66. Maini, R. and Aggarwal, H. (2010). A comprehensive review of image enhancement techniques, *arXiv preprint arXiv:1003.4053*.
67. Mehmood, I., Sajjad, M., Muhammad, K., Shah, S. I. A., Sangaiah, A. K., Shoaib, M. and Baik, S. W. (2019). An efficient computerized decision support system for the analysis and 3d visualization of brain tumor, *Multimedia Tools and Applications* 78(10): 12723–12748.
68. Menze, B. H., Jakab, A., Bauer, S., Kalpathy-Cramer, J., Farahani, K., Kirby, J., Burren, Y., Porz, N., Slotboom, J., Wiest, R. et al. (2014). The multimodal brain tumor image segmentation benchmark (brats), *IEEE transactions on medical imaging* 34(10): 1993–2024.
69. Milletari, F., Navab, N. and Ahmadi, S.-A. (2016). V-net: Fully convolutional neural networks for volumetric medical image segmentation, *2016 fourth international conference on 3D vision (3DV)*, IEEE, pp. 565–571.
70. Mishra, S. (2021). Deep transfer learning-based framework for covid-19 diagnosis using chest ct scans and clinical information, *SN Computer Science* 2(5): 1–11.
71. Mittal, L., Kumari, A., Srivastava, M., Singh, M. and Asthana, S. (2020). Identification of potential molecules against covid-19 main protease through structure-guided virtual screening approach, *Journal of Biomolecular Structure and Dynamics* pp. 1–19.
72. Muneer, K. A. and Joseph, K. P. (2018). Performance analysis of combined k-mean and fuzzy-c-mean segmentation of mr brain images, *Computational Vision and Bio Inspired Computing*, Springer, pp. 830–836.
73. Mzoughi, H., Njeh, I., Wali, A., Slima, M. B., BenHamida, A., Mhiri, C. and Mahfoudhe, K. B. (2020). Deep multi-scale 3d convolutional neural network (cnn) for mri gliomas brain tumor classification, *Journal of Digital Imaging* 33: 903–915.
74. Ozturk, S. (2020). Stacked auto-encoder based tagging with deep features for content-based medical image retrieval, *Expert Systems with Applications* 161: 113693.
75. Ogawa, S., Lee, T.-M., Kay, A. R. and Tank, D. W. (1990). Brain magnetic resonance imaging with contrast dependent on blood oxygenation, *proceedings of the National Academy of Sciences* 87(24): 9868–9872.
76. Nabizadeh, N. and Kubat, M. (2017). Automatic tumor segmentation in single-spectral mri using a texture-based and contour-based algorithm, *Expert systems with applications* 77: 1–10.
77. Patro, S. and Sahu, K. K. (2015). Normalization: A preprocessing stage, *arXiv preprint arXiv:1503.06462*. Pereira, S., Pinto, A., Alves, V. and Silva, C. A. (2016). Brain tumor segmentation using convolutional neural networks in mri images, *IEEE transactions on medical imaging* 35(5): 1240–1251.
78. Pinto, A., Pereira, S., Correia, H., Oliveira, J., Rasteiro, D.M. and Silva, C.A., 2015, August. Brain tumour segmentation based on extremely randomized forest with high-level features. In *2015 37th annual international conference of the IEEE engineering in medicine and biology society (EMBC)* (pp. 3037-3040). IEEE.
79. Pillai, J. J. (2010). The evolution of clinical functional imaging during the past 2 decades and its current impact on neurosurgical planning, *American Journal of Neuroradiology* 31(2): 219–225.
80. Pitchai, R., Supraja, P., Victoria, A. H. and Madhavi, M. (2021). Brain tumor segmentation using deep learning and fuzzy k-means clustering for magnetic resonance images, *Neural Processing Letters* 53(4): 2519–2532.
81. Politis, D. N., Romano, J. P. and Wolf, M. (1999). *Subsampling*, Springer Science & Business Media.
82. Provenzale, J. M., Mukundan, S. and Barboriak, D. P. (2006). Diffusion-weighted and perfusion mr imaging for brain tumor characterization and assessment of treatment response, *Radiology* 239(3): 632–649.
83. Punn, N. S. and Agarwal, S. (2021). Multi-modality encoded fusion with 3d inception u-net and decoder model for brain tumor segmentation, *Multimedia Tools and Applications* 80(20):30305–30320.
84. Rajini, N. H., Narmatha, T. and Bhavani, R. (2012). Automatic classification of mr brain tumor

images using decision tree, Proceedings of international conference on electronics, Vol. 31.

85. Rao, C. S. and Karunakara, K. (2021). A comprehensive review on brain tumor segmentation and classification of mri images, *Multimedia Tools and Applications* pp. 1–33
86. Rehman, A., Naz, S., Razzak, M. I., Akram, F. and Imran, M. (2020). A deep learning-based framework for automatic brain tumors classification using transfer learning, *Circuits, Systems, and Signal Processing* 39(2): 757–775.
87. Roy, S., Carass, A. and Prince, J. L. (2013). Patch based intensity normalization of brain mr images, 2013 IEEE 10th International Symposium on Biomedical Imaging, IEEE, pp. 342–345.
88. Segmentation, M.-M. G. and versus Machine, M. (2015). The multimodal brain tumor image segmentation benchmark (brats), *IEEE transactions on medical imaging* 34(10): 1993. Sharif, M. I., Khan, M. A., Alhussein, M., Aurangzeb, K. and Raza, M. (2021). A decision support system for multimodal brain tumor classification using deep learning, *Complex & Intelligent Systems* pp. 1–14.
89. Simonyan, K. and Zisserman, A. (2014). Very deep convolutional networks for large-scale image recognition, arXiv preprint arXiv:1409.1556 .
90. SUBRAMANIAN, P., LEERAR, K. F., AHAMMED, K. H., SARUN, K. and MOHAMMED, Z. (n.d.). Image registration methods.
91. Sun, X., Shi, L., Luo, Y., Yang, W., Li, H., Liang, P., Li, K., Mok, V. C., Chu, W. C. and Wang, D. (2015). Histogram- based normalization technique on human brain magnetic resonance images from different acquisitions, *Biomedical engineering online* 14(1): 1–17.
92. Tiwari, A., Srivastava, S. and Pant, M. (2020). Brain tumor segmentation and classification from magnetic resonance images: Review of selected methods from 2014 to 2019, *Pattern Recognition Letters* 131: 244–260.
93. Tustison, N. J., Avants, B. B., Cook, P. A., Zheng, Y., Egan, A., Yushkevich, P. A. and Gee, J. C. (2010). N4itk: improved n3 bias correction, *IEEE transactions on medical imaging* 29(6):1310–1320.
94. Vaishnav, K. and Amshakala, K. (2015). An automated mri brain image segmentation and tumor detection using som-clustering and proximal support vector machine classifier, 2015 IEEE International Conference on Engineering and Technology (ICETECH), IEEE, pp. 1–6.
95. Verma, H., Agrawal, R. and Sharan, A. (2016). An improved intuitionistic fuzzy c-means clustering algorithm incorporating local information for brain image segmentation, *Applied Soft Computing* 46: 543–557.
96. Vijayakumar, T. (2020). Posed inverse problem rectification using novel deep convolutional neural network, *Journal of Innovative Image Processing (JIIP)* 2(03): 121–127. Villanueva-Meyer, J. E., Mabray, M. C. and Cha, S. (2017). Current clinical brain tumor imaging, *Neurosurgery* 81(3): 397–415.
97. Villringer, A., Rosen, B. R., Belliveau, J. W., Ackerman, J. L., Lauffer, R. B., Buxton, R. B., Chao, Y.-S., Wedeenand, V. J. and Brady, T. J. (1988). Dynamic imaging with lanthanide chelates in normal brain: contrast due to magnetic susceptibility effects, *Magnetic resonance in medicine* 6(2): 164–174.
98. Wang, J., Luan, Z., Yu, Z., Gao, J., Ren, J., Khan, K., Yuan, K. and Xu, H. (2021). An adaptive sparse bayesian model combined with joint information-based label fusion For brain tumor segmentation in mri, *Signal, Image and Video Processing* pp. 1–9.
99. Warach, S., Li, W., Ronthal, M. and Edelman, R. R. (1992). Acute cerebral ischemia: evaluation with dynamic contrast-enhanced mr imaging and mr angiography., *Radiology* 182(1): 41–47.
100. Warfield, S. K., Zou, K. H. and Wells, W. M. (2004). Simultaneous truth and performance level estimation (staple): an algorithm for the validation of image segmentation, *IEEE transactions on medical imaging* 23(7): 903–921.
101. Wu, W., Chen, A. Y., Zhao, L. and Corso, J. J. (2014). Brain tumor detection and segmentation in a crf (conditional random fields) framework with pixel-pairwise affinity and superpixel-level features, *International journal of computer assisted radiology and surgery* 9(2): 241–253.
102. Xiong, H., Pandey, G., Steinbach, M. and Kumar, V. (2006). Enhancing data analysis with noise removal, *IEEE Transactions on Knowledge and Data Engineering* 18(3): 304–319.
103. Zeiler, M. D., Taylor, G. W. and Fergus, R. (2011). Adaptive deconvolutional networks for mid and high level feature learning, 2011 International Conference on Computer Vision, IEEE, pp. 2018–2025.
104. Zeineldin, R. A., Karar, M. E., Coburger, J., Wirtz, C. R. and Burgert, O. (2020). Deepseg: deep neural network framework for automatic brain tumor segmentation using magnetic resonance flair images, *International journal of computer assisted radiology and surgery* 15(6): 909–920.
105. Zhang, W., Wu, Y., Yang, B., Hu, S., Wu, L. and Dhelimd, S. (2021). Overview of multi-modal brain tumor mr image segmentation, *Healthcare*, Vol. 9, Multidisciplinary Digital Publishing Institute, p. 1051.
106. Zijdenbos, A. P., Forghani, R. and Evans, A. C. (2002). Automatic “ pipeline” analysis of 3- d mri data for clinical trials: application to multiple sclerosis, *IEEE transactions on medical imaging* 21(10): 1280–1291.
107. Zollner, F. G., Emblem, K. E. and Schad, L. R. (2010). Support vector machines in dsc-based glioma imaging: suggestions for optimal characterization, *Magnetic resonance in medicine* 64(4):1230–1236.
108. Fatima Zulfiqar, Usama Ijaz Bajwa, Yasar Mehmood, Multi-class classification of brain tumor types from MR images using EfficientNets, *Biomedical Signal Processing and Control*, Volume 84, 2023, 104777, ISSN 1746-8094
109. McBride, D.W., Szu, J.I., Hale, C., Hsu, M.S., Rodgers, V.G. and Binder, D.K., 2014. Reduction of cerebral edema after traumatic brain injury using an osmotic transport device. *Journal of neurotrauma*, 31(23), pp.1948-1954.
110. Kumar, R.L., Kakarla, J., Isunuri, B.V. and Singh, M., 2021. Multi-class brain tumor classification using residual network and global average pooling. *Multimedia Tools and Applications*, 80(9), pp.13429-13438.
111. Kaur, Gurkarandesh & Oberoi, Ashish. (2019). Novel Approach for Brain Tumor Detection Based on Naïve Bayes Classification. 10.1007/978-981-32-9949-8 31.
112. Angulakshmi, M. and Lakshmi Priya, G.G., 2017. Automated brain tumour segmentation techniques—a review. *International Journal of Imaging Systems and Technology*, 27(1), pp.66-77.
113. Leece, R., Xu, J., Ostrom, Q.T., Chen, Y., Kruchko, C. and Barnholtz-Sloan, J.S., 2017. Global incidence of malignant brain and other central nervous system tumors by histology, 2003–2007. *Neuro-oncology*, 19(11), pp.1553-1564.
114. Kumar, S., Negi, A., Singh, J.N. and Verma, H., 2018, December. A deep learning for brain tumor MRI images semantic segmentation using FCN. In 2018 4th International Conference on Computing Communication and Automation (ICCCA) (pp. 1-4). IEEE.

115. Melin, P., Gonzalez, C.I., Castro, J.R., Mendoza, O. and Castillo, O., 2014. Edge-detection method for image processing based on generalized type-2 fuzzy logic. *IEEE transactions on fuzzy systems*, 22(6), pp.1515-1525.
116. Xie, S. and Tu, Z., 2015. Holistically-nested edge detection. In *Proceedings of the IEEE inter- national conference on computer vision* (pp. 1395-1403).
117. Havaei, M., Jodoin, P.M. and Laroche, H., 2014, August. Efficient interactive brain tumor segmentation as within-brain kNN classification. In *2014 22nd international conference on pat-tern recognition* (pp. 556-561). IEEE.
118. Cui, G., Jeong, J.J., Lei, Y., Wang, T., Liu, T., Curran, W.J., Mao, H. and Yang, X., 2019, March. Machine-learning-based classification of Glioblastoma using MRI-based radiomic fea- tures. In *Medical imaging 2019: computer-aided diagnosis* (Vol. 10950, pp. 1063-1068). SPIE.
119. Li, B., Wu, C., Chi, J., Yu, X. and Wang, G., 2020, July. A deeply supervised convolutional neural network for brain tumor segmentation. In *2020 39th Chinese Control Conference (CCC)* (pp. 6262-6267). IEEE.
120. Zhang, J., Zeng, J., Qin, P. and Zhao, L., 2021. Brain tumor segmentation of multi-modality MR images via triple intersecting U-Nets. *Neurocomputing*, 421, pp.195-209.
121. Balwant, M.K., 2022. A review on convolutional neural networks for brain tumor segmentation: methods, datasets, libraries, and future directions. *Irbm*, 43(6), pp.521-537.
122. Hatamizadeh, A., Nath, V., Tang, Y., Yang, D., Roth, H.R. and Xu, D., 2021, September. Swin unetr: Swin transformers for semantic segmentation of brain tumors in mri images. In *Interna- tional MICCAI Brainlesion Workshop* (pp. 272-284). Cham: Springer International Publishing.
123. Li, G., Li, L., Li, Y., Qian, Z., Wu, F., He, Y., Jiang, H., Li, R., Wang, D., Zhai, Y. and Wang, Z., 2022. An MRI radiomics approach to predict survival and tumour-infiltrating macrophages in gliomas. *Brain*, 145(3), pp.1151-1161.
124. Crimi, A., Bakas, S., Kuijf, H., Keyvan, F., Reyes, M. and van Walsum, T. eds., 2019. *Brainle- sion: Glioma, Multiple Sclerosis, Stroke and Traumatic Brain Injuries: 4th International Work- shop, BrainLes 2018, Held in Conjunction with MICCAI 2018, Granada, Spain, September 16,2018, Revised Selected Papers, Part II* (Vol. 11384). Springer.
125. Naz, A.R.S., Naseem, U., Razzak, I. and Hameed, I.A., 2019. Deep autoencoder-decoder frame- work for semantic segmentation of brain tumor. *Aust. J. Intell. Inf. Process. Syst*, 15(4).
126. Pino, M.A., Imperato, A., Musca, I., Maugeri, R., Giammalva, G.R., Costantino, G., Graziano, F., Meli, F., Francaviglia, N., Iacopino, D.G. and Villa, A., 2018. New hope in brain glioma surgery: the role of intraoperative ultrasound. *A review. Brain sciences*, 8(11), p.202.

